



## Rice Husk Ash /Sodium Alginate Beads as Effective Adsorbent for Heavy Metals and Fluoride I

khalid M. khader<sup>1</sup>, Rabie S. Farag<sup>1</sup>, Mostafa M. S. Abo-Elfadl<sup>2</sup>, Mohamed E. A. ali<sup>2</sup>

<sup>1</sup>Chemistry Department, Faculty of Science, Al-Azhar University, Cairo, Egypt.

<sup>2</sup>Desert Research Center, Cairo, Egypt.



CrossMark

### Abstract

Rice husk ash (RHAB) blended with sodium alginate was prepared and used for the adsorption of some heavy metals ( $\text{Cu}^{2+}$ ,  $\text{Ni}^{2+}$ ,  $\text{Mn}^{2+}$ ,  $\text{pb}^{2+}$ ), fluoride ion ( $\text{F}^-$ ) and turbidity of polluted surface water resources. The removal rate for each element occurred at the optimum dose (5 g/l) with removal efficiencies of 95, 78, 84, 98, and 95 % for  $\text{Cu}^{2+}$ ,  $\text{Ni}^{2+}$ ,  $\text{Mn}^{2+}$ ,  $\text{pb}^{2+}$  and  $\text{F}^-$ , respectively. The maximum sorption capacity ( $Q_{\text{max}}$ ) to RHAB of (12.5, 8, 8.3, 13, and 13 mg/g) and (12.7, 8.4, 9, 13.3, and 13.1 mg/g) were reported for ( $\text{Cu}^{2+}$ ,  $\text{Ni}^{2+}$ ,  $\text{Mn}^{2+}$ ,  $\text{pb}^{2+}$ , and  $\text{F}^-$ , respectively). The results showed that turbidity, heavy metals, and fluoride ion removal were dependent on pH, coagulant dosing, mixing, and concentration, as well as the initial turbidity of water for both used coagulants. Biosorbents that can remove heavy metals, turbidity, and fluoride from wastewater are expected to be good at this. RHAB is one of them.

Keywords; Rice husk ash beads; Heavy metals and fluoride ion removal; Adsorption isotherms; Reusability; Water

### 1. Introduction

Pollution of surface and groundwater from agriculture, domestic and industrial activities has not been regularly monitored and recorded as a problem. This may be due to the absence of a problem or the lack of monitoring facilities in the Pacific Island countries [1]. Water contamination by heavy metals has been a major concern for researchers and government agencies involved with pollution control [2], mainly by toxic heavy metals and harmful contaminants due to their ability to retain and accumulate in the human body [3]. Heavy metals contaminate surface and ground water, affecting the quality of water as these metals are persistent, toxic, and dangerous to humans [4,5]. Adsorption using bio-sorbents, including agricultural by-products, has been found to be an attractive process for the removal of pollutants, especially organic materials, from

industrial effluents [6,7]. A variety of agricultural by-products, such as cocoa shell [8,9], coconut shell [10], pomegranate peel waste [11], cashew nut shell [12], orange peel [13], rice husk [14,15], etc., have been used as adsorbents for the removal of different contaminants from aqueous solutions. However, such bio-sorbents' low absorption capacity has limited their utility in the removal of contaminants from water. To overcome this problem, agricultural by-products can be transformed into biochar or activated carbons, which have higher surface area and adsorption capacities [16]. For instance, among the mentioned agricultural wastes, rice husk has been used as activated carbon to clean the environment from contaminants because it has been reported as a good adsorbent to remove many contaminants [17]. In conventional or modified form, rice husk ash (RHA) has been shown to be very effective in the adsorption of active dyes [18], arsenic [18], heavy metal ions [19], phenol [20], bisphenol [21],

\*Corresponding author e-mail: [\\*E-mail: khalidmahmoudkhader@gmail.com](mailto:khalidmahmoudkhader@gmail.com) (Khalid Khader)

Received date 09 January 2022; revised date 10 February 2022; accepted date 13 February 2022

DOI: 10.21608/ejchem.2022.115427.5236

©2023 National Information and Documentation Center (NIDOC)

phosphate [22], etc. from aqueous solutions. The adsorption capacity of adsorbents strongly depends on the activation method and the conditions of production [23]. Rice husk is a by-product of the rice milling process. Rice husk ash is a solid obtained after the burning of rice husks [24]. Under various experimental conditions, SiO<sub>2</sub> nanoparticles were prepared after the extraction of sodium silicate from RHA and used for the removal of Fe<sup>2+</sup> ions from aqueous solutions [25].

The ability of rice husk ash beads to remove heavy metal ions from the simulated synthesized aqueous solution in a batch mode was investigated. Various parameters were investigated, including the pH of the simulated synthesized aqueous solution of the selected heavy metal ion, the adsorbent dose, initial metal ion concentration, re-usability of adsorbent matter, and the contact time of treatment (t). The experiments were undertaken by varying all the above parameters for different initial concentrations (C<sub>0</sub>) of selected simulated synthesized aqueous solutions of heavy metals tested individually. The results thus obtained are explained below. In this study, we used calcium alginate beads of treated RHAB as natural bio-sorbents to determine their efficiencies to reduce metal ions such as Cu<sup>2+</sup>, Ni<sup>2+</sup>, Mn<sup>2+</sup>, pb<sup>2+</sup>, and F<sup>-</sup> in synthetic water. Their effectiveness was evaluated at different pH values, mixing times, initial metal ion concentrations, and bio-sorbent dosages to find the optimal operational conditions for maximum metal ion removal in a water treatment plant.

## 2. MATERIALS AND METHODS

### 2.1. Preparation of RHA.

Rice husk was partially carbonized at 250°C to 300 °C in oven for duration of 4 to 5 hours, and then it is completely carbonized in a muffle furnace at temperature 500°C to 600 °C then, and it was cooled to room temperature. A post that it was then washed repeatedly with hot boiling water so as to open the pores of carbon. Completely carbonized rice husk was further treated by acid treatment. Rice husk biomass, mixed with IN of HNO<sub>3</sub> in 1: 1 ratio, was taken in a 1000 ml conical flask. The mixture then was molded and heated to 600°C to 700°C in a muffle furnace. Treated biomass was washed with distilled water until the maximum color was removed and clear water obtained.

### 2.2. Rice husk ash bead formation (RHAB).

The Rice husk ash was washed with de-ionized water, air-dried, and the pulverization process was carried out to get a fine powder, which was encapsulated by cross-linked polymerization of sodium alginate and calcium chloride. In order to improve the properties of the RHA, the powdered alginate was dissolved in a phosphate-buffered saline

solution to form a viscous solution with different concentrations (varying from 1–3%). After mixing 1:3 ratios of the RHA powder and viscous solution, they are allowed to fall drop wise in 2.5% (w/v) sterile calcium chloride solution with the help of a peristaltic pump. The flow rate of the pump was adjusted to be 200 spherical beads per hour. After encapsulation, the beads in the salt solution were incubated at room temperature for 2 h for the complete replacement of ions [26, 27].

### 2.3. Characterization

The IR analysis of Rice husk ash and its beads were analyzed with a FTIR spectrophotometer (Shimadzu FTIR-8400, Japan). All the samples were crushed with potassium bromide to get pellets at 600 kg cm<sup>-2</sup>. Spectral scanning was done in the range of 400–4000 cm<sup>-1</sup>. The spectral range varied between 4000 to 500 cm<sup>-1</sup>, with twenty eight scans in a resolution of 4 cm<sup>-1</sup>. The surface morphology was studied by using a scanning electron microscope (model JEOL JSM-6360, Japan).

### 2.4. Batch Adsorption Studies.

Sorption tests were conducted at 100 rpm [28] by batch technique on jar test equipment (Model Flocumatic, J.P Selecta, Spain). To elucidate the influence of certain parameters on the sorption of Cu<sup>2+</sup>, Ni<sup>2+</sup>, Mn<sup>2+</sup>, pb<sup>2+</sup> and F<sup>-</sup> ions into RHAB, batch tests were administered. Those parameters investigated included pH, adsorbent dosage, concentration of metal ions, and contact time. All adsorption tests were conducted at pH 5, with HCl (1N) and NaOH (1N) solutions, agitation time 160 rpm for 3h and sorbent dose (5 g/l). All adsorption tests were performed in a 100 ml solution with a metal ion concentration of 50 ppm. Batch tests were conducted for various metal concentrations (10, 25, 75, and 100 mg/l), contact time (15-250 min), adsorbent dosage (1-5 g) and pH (2-8) in order to establish the optimal experimental conditions. The initial and final ion concentrations were calculated using AAS. The amount of the metal adsorbed (% removal) by the sorbent was calculated using Eqn. 1.

$$\% \text{ Removal Efficiency} = ((C_i - C_f) / C_i) \times 100 \quad \text{Eqn. 1}$$

The amount of adsorbed metal ions onto the surface of the adsorbent was calculated from the mass balance expression given by Eqn. 2:

$$q_e = \frac{(C_i - C_f)}{M} V \quad \text{Eqn. 2}$$

where, q<sub>e</sub> is the amount of metal ions adsorbed (mg/g); C<sub>i</sub> initial metal ion concentration (mg/L), C<sub>f</sub> is the final metal ion concentration (mg/L), M is the mass of the adsorbent in (g), and V is the volume (liter) of the metal solution in contact with the

adsorbent.

### 2.5. Adsorption isotherms.

The adsorption isotherm models of Langmuir [29] and Freundlich [30] were used. For Langmuir model the linear form could be expressed by the following equation:

$$\frac{C_e}{q_e} = \frac{1}{K_L q_{max}} + \frac{C_e}{q_{max}} \quad \text{Eqn. 3}$$

The Freundlich model, the linear form could be expressed from the following equation:

$$\log q_e = \log k_F + (1/n) \log C_e \quad \text{Eqn. 4}$$

where  $C_e$  is the equilibrium concentration of metal in mg/l,  $q_e$  and  $q_m$  are the adsorped amount at equilibrium (mg/g) and adsorption capacity (mg/g), respectively, and  $K_L$  is the Langmuir constant (L/mg). The values of  $K_L$  and  $q_m$  can be obtained from the intercept and slope of  $C_e/q_e$  versus  $C_e$ .  $K_F$  is the empirical Freundlich constant (mg/g) and  $1/n$  is the Freundlich exponent.

To predict whether an adsorption system is favorable or unfavorable, the equilibrium parameter ( $R_L$ ) was calculated according to the following equation 5:

$$R_L = 1/(1 + bC_e) \quad \text{Eqn. 5}$$

where  $b$  is the Langmuir constant (l/mg) and  $C_f$  is the final concentration (mg/l) in the solution, if  $R_L > 1$  the isotherm is unfavorable, whereas if  $R_L < 1$  the isotherm is favorable.

### 2.6. Adsorption Kinetics

The pseudo-first-order kinetic model [31] and pseudo-second-order kinetic model [32], were employed to fit the experimental data and to understand the adsorption mechanism of  $Cu^{+2}$ ,  $Ni^{+2}$ ,  $Mn^{+2}$ ,  $Pb^{+2}$ , and  $F^-$  ions onto the surface of RHAB as adsorbent matter. The equation of Pseudo-first-order kinetic model is as follows:

$$\log (q_e - q_t) = \log q_e - ((k_1/2.303) * t) \quad \text{Eqn. 6}$$

where  $q_t$  and  $q_e$  (mg /g) are the amounts of metal ions adsorbed per unit mass of the adsorbent at time  $t$  (min) and equilibrium, respectively, and  $k_1$  (1/min) is the pseudo-first-order rate constant of the sorption process. The equation of Pseudo-second-

order kinetic model is as follows:

$$t/q_t = 1/k_2 q_e^2 + t/q_e \quad \text{Eqn. 7}$$

Where  $k_2$  [g/ (mg min)] is the pseudo-second-order rate constant.

### 2.7. Desorption experiment.

Sorption studies, removal studies using standard  $Cu^{2+}$ ,  $Ni^{2+}$ ,  $Mn^{2+}$ ,  $Pb^{2+}$  and  $F^-$  solutions were carried out in triplicate. Constant dose 5 g/l of beads were shaken with 50ml of polluted water solution of 50 ppm for different time (min) using a magnetic agitator and then the suspension was filtered using filter paper (Whatman 42, 28  $\mu$ m). The adsorbent material used in the isotherms was separated from the aqueous solution by filtration, washed with distilled and deionized water, and dried in oven at  $60 \pm 2$  °C for 24 h. The mass of adsorbent obtained was placed in contact with 100 ml of HCl (37%) at 0.1 N and stirred at 250 rpm at 25 °C for 120 min. After this step, the metal concentration in the solution was determined by FAAS, and the desorption percentage was calculated by Eqn. 8:

$$D = \frac{C_{e_{des}}}{C_{e_{ads}}} * 100 \quad \text{Eqn. 8}$$

where  $C_e$  (des) (mg/l) and  $C_e$  (ads) (mg/l) are the metal ions concentrations desorbed by Rice husk beads and that adsorbed at equilibrium, respectively.

## 3. RESULTS AND DISCUSSION

### 3.1. Characterization of the bio-sorbent material.

#### 3.1.1. Scanning electron microscopy (SEM) of bio-sorbent.

Fig.1 Shows SEM of Rice ash surface (RH) burned at 700 °C, 900 °C, and a rice ash powder blended with sodium alginate (RHAB), respectively. The structure for 900 °C seemed to be highly porous. Moreover, the uniformed arrangement with both small and large grains was also visible in this case. On the other hand, a uniform pattern with the least amount of pore was confirmed by the SEM micrograph sintered at 700 °C. SEM image of RAHB showed strongly influenced of SA on the manifestation of microstructure, which increases the surface roughness and hence leads to improving the bio-sorption process.

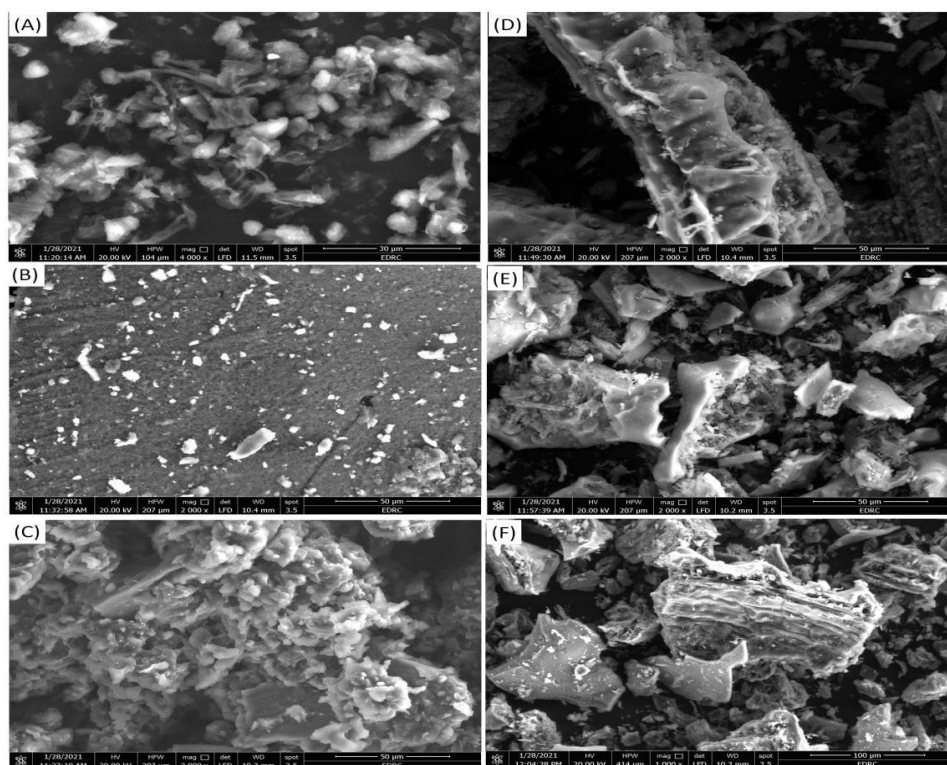


**Fig. 1:** The surface morphology of RH burned at 700 °C (D), RH burned at 900 °C (E), and RHAB (F)

### 3.1.2. Fourier Transform Infrared spectroscopy spectrum (FTIR)

FTIR spectroscopy is a valuable tool in examining the presence of certain functional groups in a molecule, since each particular chemical bond shows a unique energy absorption band [33]. Therefore, functional groups responsible for the removal of a contaminant could be determined by analyzing the variation on the spectra of the RHAB to show their functional groups responsible adsorption process. The results of FTIR analysis of raw rice husk ash were shown in Fig. 2. The spectra are recorded between 4000  $\text{cm}^{-1}$  and 500  $\text{cm}^{-1}$ . Rice husk contains cellulose, hemicellulose, lignin and waxes that most likely consist of alkene, esters, aromatic, ketones and alcohols with oxygen containing different functional groups. From Fig. 2 the broadband appeared at 1042  $\text{cm}^{-1}$  ascribed the bending vibration  $-\text{CH}_3$  [34]. Spectral analyses were conducted for carbonized RHA at 700 °C (A), carbonized RHAB (CRHAB) at 900 °C (B), and sodium alginate beads (C) to identify any changes occurred on the spectrum profile due to interaction between CRHAB and SA. Fig. 2 shows the IR spectrum of CRHA, which displayed significant peaks in the region between 400  $\text{cm}^{-1}$  to 1100  $\text{cm}^{-1}$  are probably due to the silicon atom attached to the oxygen in the rice husk ash. After treating the rice husk ash with chemical agent, some of the functional

group's disappeared. This is due to the functional groups reaction with NaOH and its subsequent removal by water. Next, we can find that after carbonizing the rice husk in a  $\text{N}_2$  atmosphere, the spectrum of CRH sample is different from the raw material. Many bands disappeared after carbonization which indicates the vaporization of organic matter. This could be explained by the fact that in the carbonization process with  $\text{N}_2$ , moisture and volatile matters were removed from the material. The strong and high intensity peaks of CRHAB which appeared at 400  $\text{cm}^{-1}$  to 1100  $\text{cm}^{-1}$  are assigned to the silicon atom attached to the oxygen in the rice husk ash. This result indicates that the RHAB consist of various functional groups that play important role in the adsorption of contaminants from polluted water.

Generally, FTIR spectra for both CRHA and CRHB blended with sodium alginate were found to be nearly identical (fig. 2). The changes in the peak intensities together with the slight shift of wavenumbers were observed, especially between 400  $\text{cm}^{-1}$  to 1100  $\text{cm}^{-1}$ . Slight alterations of peak intensities were noticed on the FTIR spectra profile of CRHAB compared with the spectra of the pure CRH along the studied wavenumbers (Fig. 2). Based on this result, it is suggested that specific functional groups such as  $\text{SiO}_2$  involve in the removal of heavy metal ions, fluoride ions, and turbidity molecules from contaminated water.

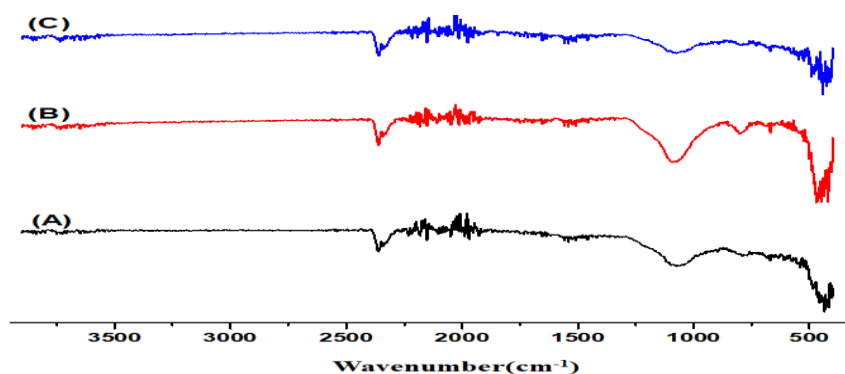


**Fig. 2:** FTIR spectra for both carbonized RHA at 700C° (A), carbonized RHAB (CRHAB) at 900C° (B), and sodium alginate beads (C)

### 3.2. Effect of adsorbent dose

The effect of bio-sorbent dosage of RHAB is one of the most important parameters that should be considered to determine the optimum condition in bio-sorption process. Insufficient dosage of bio-sorbents can be resulted in the poor removal performance in the process. Therefore, it is significant to determine the most favorable dosage in order to minimize the treatment cost and to acquire the optimum removal efficiency cost in the treatment process [35]. The bio-sorption experiments were carried out with various doses of bio-sorbent from (1-5 g/l). Fig. 3 illustrated the effect of bio-sorbent doses of RHAB of bio-sorption process of metal ions for maximum metal ion removal (1-5 g/l) at constant pH (5-5.5) for metal ions and pH (2) for F<sup>-</sup> and mixing rate 160 rpm for 90 min. Fig. 3 Showed that the increases of bio-sorbent dose of RHAB the increases to metal ion removal, this is due to the silica group in RHAB surface is strongly reactive with metal ions particles carrying positive charges. The nitrogen atoms of amino group hold unpaired electron

doublets that can react with metal cations. Silica groups are thus responsible for the uptake of metal cations by a chelation mechanism [36, 37]. Therefore; the optimum dose of RHAB for maximum metal ion removal occurred at a constant dose (5 g/l) with removal efficiencies of 95, 78, 84, 98, 95 % for Cu<sup>2+</sup>, Ni<sup>2+</sup>, Mn<sup>2+</sup>, pb<sup>2+</sup> and F<sup>-</sup>, respectively. The results indicated that when the RHAB adsorbent doses were increased, the percentage removal of all heavy metal ions when tested individually also increased. The increase in adsorbent dose meant an increase in the amount of adsorbent media, thus increasing the surface area of adsorbent material available. This in turn increased the number of active sites in the adsorbent material surface, i.e., an increase in the availability of binding sites for adsorption and consequently increasing the heavy metal ion removal capacity of the bio-sorbent. This leads to an increase in the ability of the bio-sorbent to adsorb a greater amount of heavy metal ions from the simulated synthesized aqueous solution at different initial concentrations and ultimately the-percentage removal of all the heavy metal ions also increased.

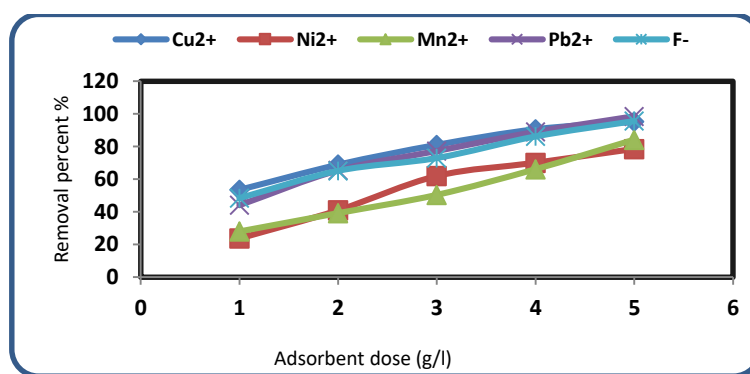


**Fig. 3:** Effect of adsorbent dose of RHAB on the percentage removal of different heavy metal ions (Cu<sup>2+</sup>, Ni<sup>2+</sup>, Mn<sup>2+</sup>, pb<sup>2+</sup>) and F<sup>-</sup>: (at C<sub>0</sub> = 50 mg/L, T = 25°C, t = 60 min and pH (5-5.5 and 2) for metal ions and F<sup>-</sup>, respectively.

### 3.3. Effect of solution pH

It is well recognized that the pH of the solution is an important parameter that affects the

adsorption of heavy metal ions [38]. The solution pH of adsorbate is the most important parameter for proper uptake, as it effects on surface charge of the adsorbent species [39]. Fig. 4 illustrated the

percentage removal of the heavy metals ( $\text{Cu}^{2+}$ ,  $\text{Ni}^{2+}$ ,  $\text{Mn}^{2+}$ ,  $\text{pb}^{2+}$ ) increased as the pH of the simulated synthesized aqueous solution increases. The lower adsorption of the heavy metals ( $\text{Cu}^{2+}$ ,  $\text{Ni}^{2+}$ ,  $\text{Mn}^{2+}$ ,  $\text{pb}^{2+}$ ) at a lower pH less than 5 can be explained both in terms of the species of the metal and the adsorbent surface. In this case, at a lower pH, i.e., acidic conditions, the surface of the RHAB as adsorbent becomes highly protonated and hence the adsorption decreases. With an increasing pH of the aqueous solution, the degree of protonation of the surface reduces gradually and hence the adsorption increases

[40]. Furthermore, as the pH decreases, there is competition between protons of the amino, carboxylic, silica groups and the metal ions, the former being the dominant species at higher pH values. The net positive surface potential of the sorbent media increases, resulting in a reduction in the electrostatic attraction between the sorbent metal ion species and the adsorbent material surface, with a consequent reduced sorption capacity which ultimately leads to a decrease in the percentage adsorption of metal ions [41].

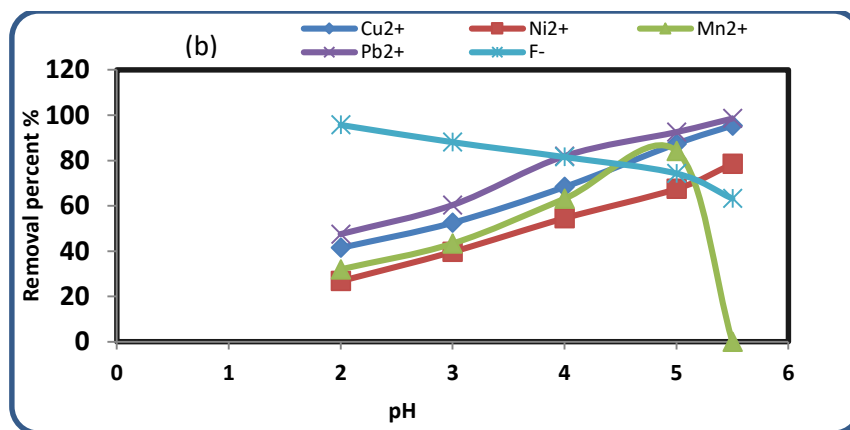


**Fig. 4:** Effect of varying pH of solution on adsorption process of RHAB for maximum metal ions ( $\text{Cu}^{2+}$ ,  $\text{Ni}^{2+}$ ,  $\text{Mn}^{2+}$ ,  $\text{pb}^{2+}$ ) and  $\text{F}^-$  removal at constant dose 5 g/l.

The most predominated species of RHAB as adsorbent at this pH value (5.0-5.2) are negatively charged that are very effective to remove most cationic metal ions  $\text{Cu}^{+2}$ ,  $\text{Ni}^{+2}$ ,  $\text{Mn}^{+2}$ ,  $\text{pb}^{+2}$  [42]. As shown in fig. 4, the optimum pH for maximum metal ions and fluoride removal using beads of RHAB as adsorbent was found to range from (5.0-5.2) for metal ions and pH 2 for fluoride with removal efficiency (95, 78, 84, 98, 95%) for  $\text{Cu}^{2+}$ ,  $\text{Ni}^{2+}$ ,  $\text{Mn}^{2+}$ ,  $\text{pb}^{2+}$  and  $\text{F}^-$ , respectively by RHAB respectively. This is due to, at optimum conditions and constant pH (5.0-5.2), an electrostatic repulsion protons of silica groups in RHAB is very low, so more active sites are available, hence no steric hindrance occurs, and electrostatic attraction increases, so the adsorption process increases, and the removal process occurs and the residual metals ion lower than the permissible limit.

In case of using RHAB as bio-sorbent for fluoride ions, the most predominated species of surface at this pH value (2-4) are positively charged that are very effective to adsorb fluoride ions [42]. As shown in (fig. 4), the optimum pH for maximum  $\text{F}^-$  ion removal using RHAB as bio-sorbent was found to range from (2-4) with removal efficiency ranging (93-95%), this is due to abruptly decreases of what became more acidic.

### 3.4. Effect of metal ions concentration

The results showed that the percentage removal of individual heavy metal ions and fluoride ions increased when the initial concentration ( $C_0$ ) of the individual heavy metal ions and fluoride were increased up to concentration 50 ppm (fig. 5). This can be explained by the fact that the initial concentration of the heavy metal ions had a restricting effect on the removal capacity whilst simultaneously the adsorbent media had a limited number of active sites, which would have become saturated at a certain concentration. This led to an increase in the number of heavy metal ion molecules competing for the available functional groups on the surface of the adsorbent material. Since a solution with a lower concentration has a smaller amount of heavy metal ions than a solution with a higher concentration, so the percentage removal decreased with increasing initial concentration of the individual heavy metal ions. For the RHAB as adsorbent material, the highest percentage removal was occurred at constant initial concentration 50 ppm, at optimum conditions with removal efficiency (95, 78, 84, 98, 95%) for  $\text{Cu}^{2+}$ ,  $\text{Ni}^{2+}$ ,  $\text{Mn}^{2+}$ ,  $\text{pb}^{2+}$  and  $\text{F}^-$ , respectively on the surface of RHAB, respectively.

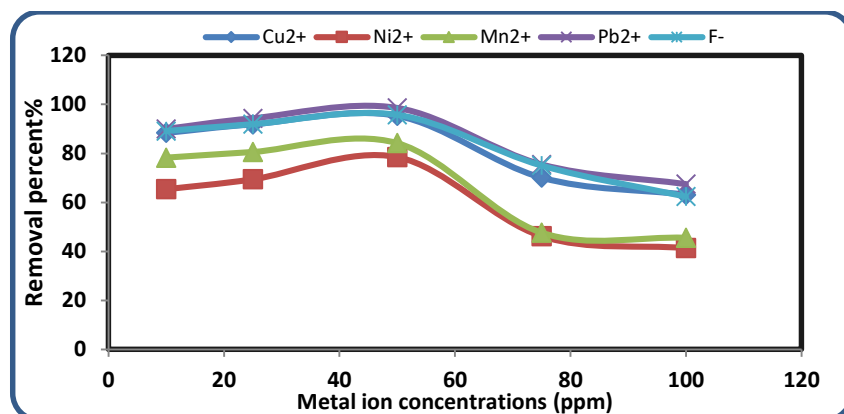


**Fig. 5:** Metal ion concentration effect on adsorption process of RHAB for maximum metal ions and fluoride removal: (at  $T = 25^{\circ}\text{C}$ , dose = 5 g/l,  $t = 60$  min and pH (5-5.5 and 2) for metal ions and  $\text{F}^-$ , respectively).

### 3.5. Effect of Contact time

In this study, the experiments were carried out at a constant mixing time 160 rpm for constant time 90 min., and at optimum conditions for both adsorbent materials. Fig. 6 showed that the optimum contact time for maximum metal ions and fluoride removal was found at 90 min for both adsorbent materials. This is due to that the adsorption process was very high, due increase contact time of mixing rate led to increase the collision between the bio-sorbent molecules and metal ion or fluoride molecules, hence more active sites are available, and so, adsorption process was increased. However; above or below the optimum contact time of mixing rate, metal ions and fluoride ions removal decreased. This is due to decrease the collision between the bio-sorbent molecules and metal ion and fluoride molecules, hence more active sites are not available,

and so the concentration of metal ions and fluoride ion of treated water begins to increase another time due adsorption process was decreased. The results indicate that when the treatment time of the simulated synthesized aqueous solution of heavy metal ions and fluoride ions were increased the percentage removal of heavy metal ions also increased when tested individually with all other variables held constant as shown in (fig. 6). So the RHAB adsorbent material can uptake a greater amount of heavy metal ions and fluoride ions from the simulated synthesized aqueous solution, therefore, the percentage removal of heavy metal ions from the aqueous solution increases. This indicated that the optimum contact time at mixing rate 160rpm for maximum metal ions and fluoride removal occurred at 90min at optimum conditions with removal efficiencies 95, 78, 84, 98, 95 % for  $\text{Cu}^{2+}$ ,  $\text{Ni}^{2+}$ ,  $\text{Mn}^{2+}$ ,  $\text{pb}^{2+}$  and  $\text{F}^-$  on RHAB, respectively.

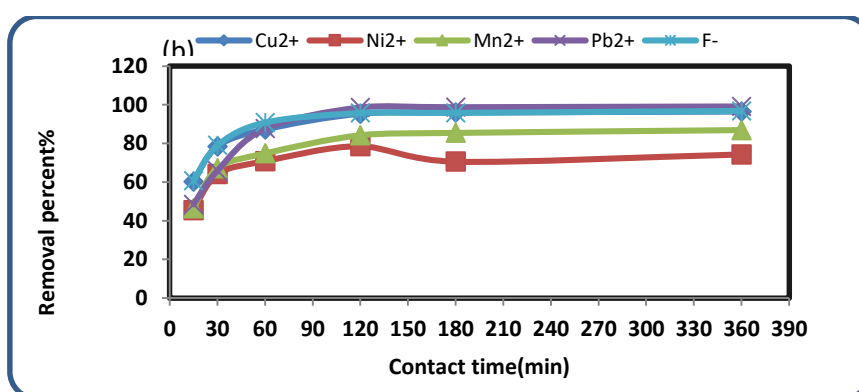


**Fig. 6:** Contact time effect on the percentage removal of different heavy metal ions of RHAB for maximum metal ions and fluoride removal: (at  $T = 25^{\circ}\text{C}$ , dose = 5 g/l,  $t = 60$  min and pH (5-5.5 and 2) for metal ions and  $\text{F}^-$ , respectively).

### 3.6. Adsorption Isotherms

The adsorption capacity of RHAB adsorbent is related to initial ion concentrations (figs. 7-11), where the adsorption capacity was increased with increasing the initial ion concentration while the removal efficiency was decreased. However, to describe the adsorption mechanism and analyze the experimental data of  $\text{Cu}^{2+}$ ,  $\text{Ni}^{2+}$ ,  $\text{Mn}^{2+}$ ,  $\text{pb}^{2+}$  and  $\text{F}^-$  ions adsorption onto RHAB adsorbent.

By comparing the correlation coefficients of the two isotherm models, it was found that all RL values of the Langmuir isotherm model fitted better than all RL values of Freundlich isotherm model, suggesting that sorption of  $\text{Cu}^{2+}$ ,  $\text{Ni}^{2+}$ ,  $\text{Mn}^{2+}$ ,  $\text{pb}^{2+}$  and  $\text{F}^-$  ions onto

RHAB adsorbent, are monolayer coverage. This might be attributed to the homogeneous distribution of the functional the silica oxide groups onto the surface of RHAB. The calculated maximum adsorption capacity of Langmuir isotherm model ( $Q_{\max} = 12.66, 8.71, 9.03, 13.33 \text{ mg/g}$ ) and 13.13) for  $\text{Cu}^{2+}$ ,  $\text{Ni}^{2+}$ ,  $\text{Mn}^{2+}$ ,  $\text{pb}^{2+}$  and  $\text{F}^-$  ions onto RHAB adsorbent respectively. From Table 1, it was illustrated that RHAB adsorbent has the highest maximum adsorption capacity compared to other adsorbents. This is due to containing the adsorbent onto multi-functional groups of RHAB (silica oxide groups), which act as chelation sites for all contaminants in polluted water.

**Table 1:** Illustrates the Langmuir and Freundlich isotherm models for the adsorption of  $\text{Cu}^{2+}$ ,  $\text{Ni}^{2+}$ ,  $\text{Mn}^{2+}$ ,  $\text{Pb}^{2+}$  and  $\text{F}^-$  onto RHAB adsorbent ( $n=3$ ).

Ions	Absorbent	Langmuir equation			Freundlich equation		
		$Q_{\max}$	$K_L$	$R^2$	$n$	$K_F$	$R^2$
$\text{Cu}^{2+}$	RHAB	12.66	0.582	0.989	2.98	4.27	0.8003
$\text{Ni}^{2+}$	RHAB	8.41	0.272	0.984	2.81	2.21	0.819
$\text{Mn}^{2+}$	RHAB	9.03	0.26	0.969	2.787	2.38	0.722
$\text{Pb}^{2+}$	RHAB	13.33	0.91	0.991	3.58	5.7	0.751
$\text{F}^-$	RHAB	13.13	0.57	0.994	2.79	4.27	0.823

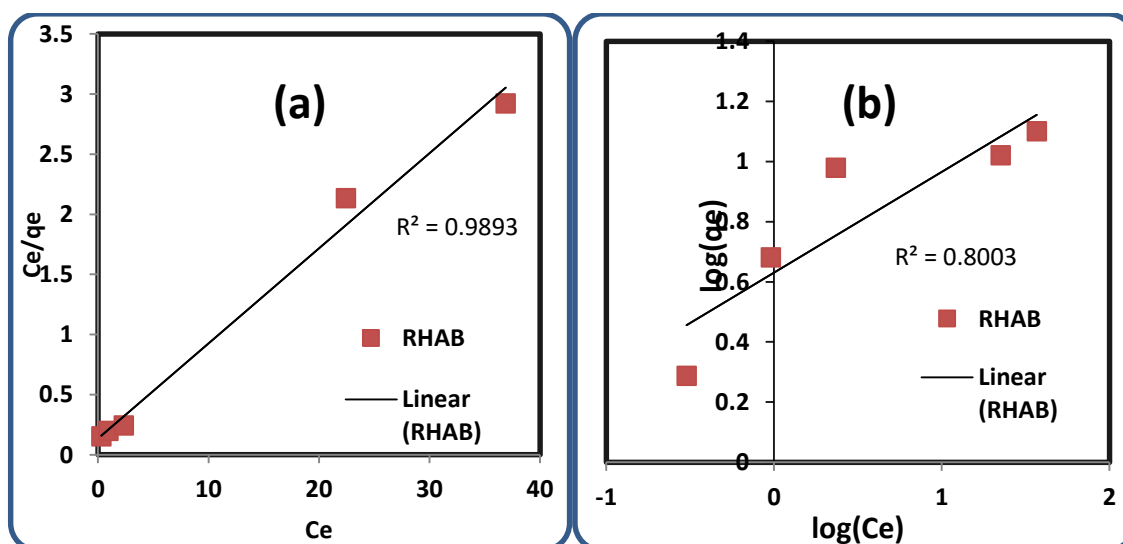


**Fig. 7:** Langmuir (a) and Freundlich (b) isotherm models for the adsorption of  $\text{Cu}^{2+}$  ions on to RHAB adsorbent respectively.

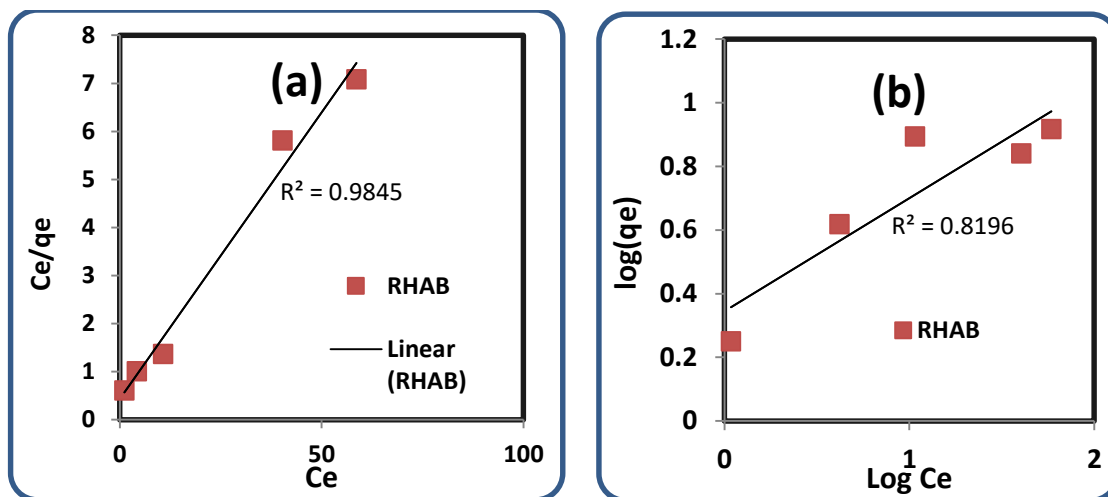


Fig. 8: Langmuir (a) and Freundlich (b) isotherm models for the adsorption of Ni<sup>2+</sup> ions on to RHAB adsorbent respectively.

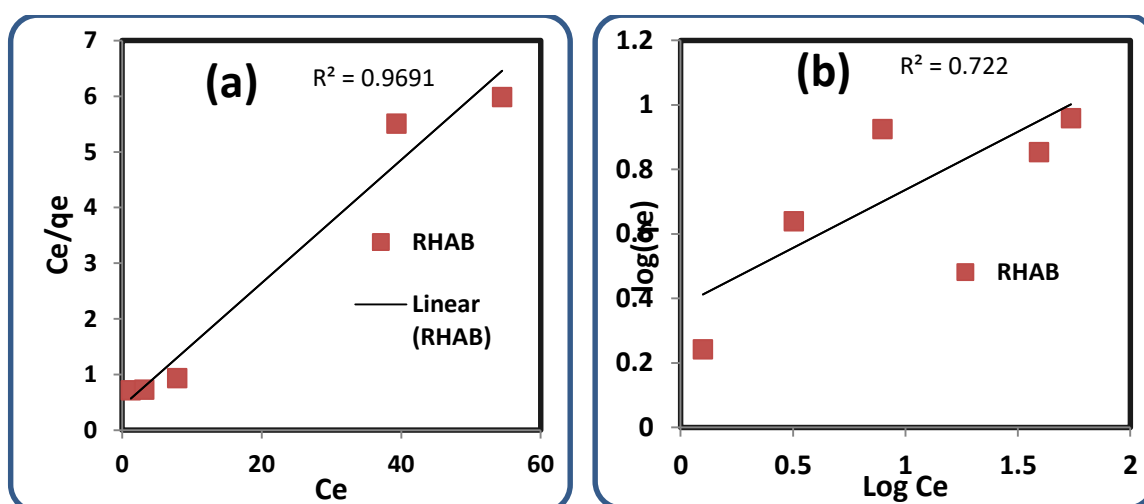


Fig. 9: Langmuir (a) and Freundlich (b) isotherm models for the adsorption of Mn<sup>2+</sup> ions onto RHAB adsorbent respectively.

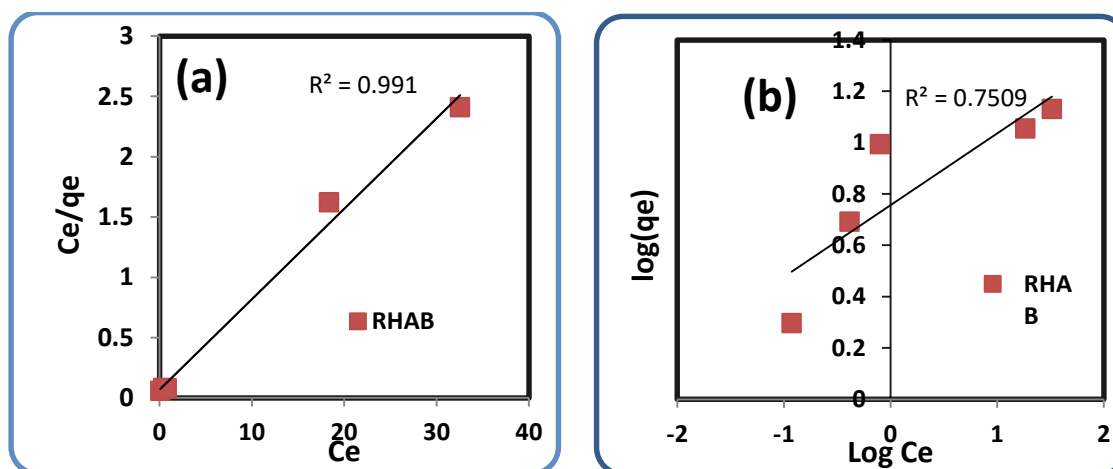


Fig. 10: Langmuir (a) and Freundlich (b) isotherm models for the adsorption of Pb<sup>2+</sup> ions onto RHAB adsorbent respectively.

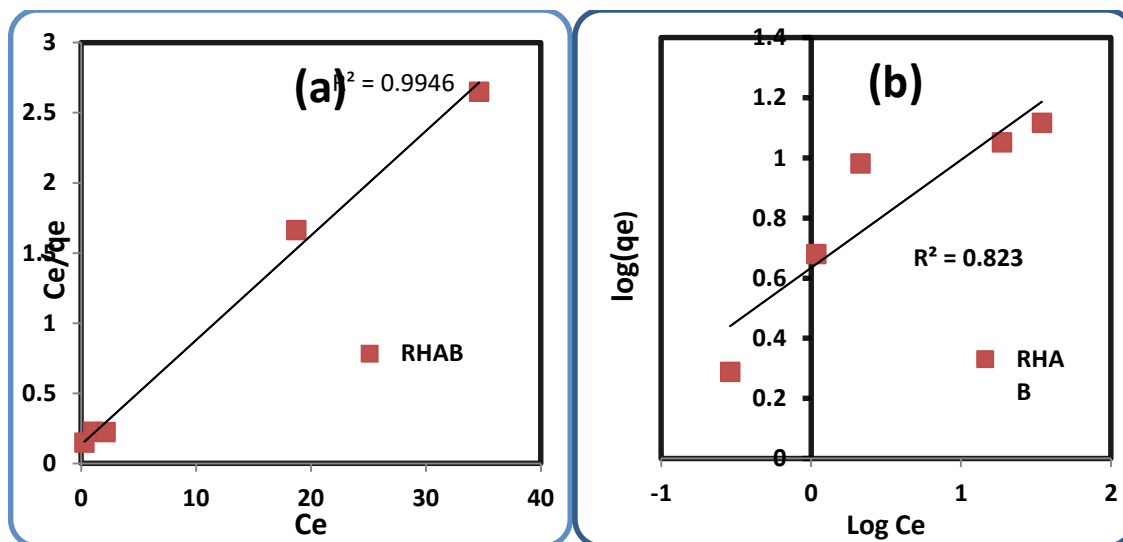


Fig. 11: Langmuir (a) and Freundlich (b) isotherm models for the adsorption of F<sup>-</sup> ions onto RHAB adsorbent respectively.

### 3.7. Adsorption Kinetics

The effect of contact time on the adsorption of Cu<sup>2+</sup>, Ni<sup>2+</sup>, Mn<sup>2+</sup>, pb<sup>2+</sup> and F<sup>-</sup> ions onto the surface of RHAB was shown in (figs. 12-16). It was observed that at contact time 90 min, the maximum removal

efficiency (97, 80, 86, 99, 97 %) for Cu<sup>2+</sup>, Ni<sup>2+</sup>, Mn<sup>2+</sup>, pb<sup>2+</sup> and F<sup>-</sup> on RHAB, respectively. After that, no significant change was observed; therefore, the optimum contact time is 90 min.

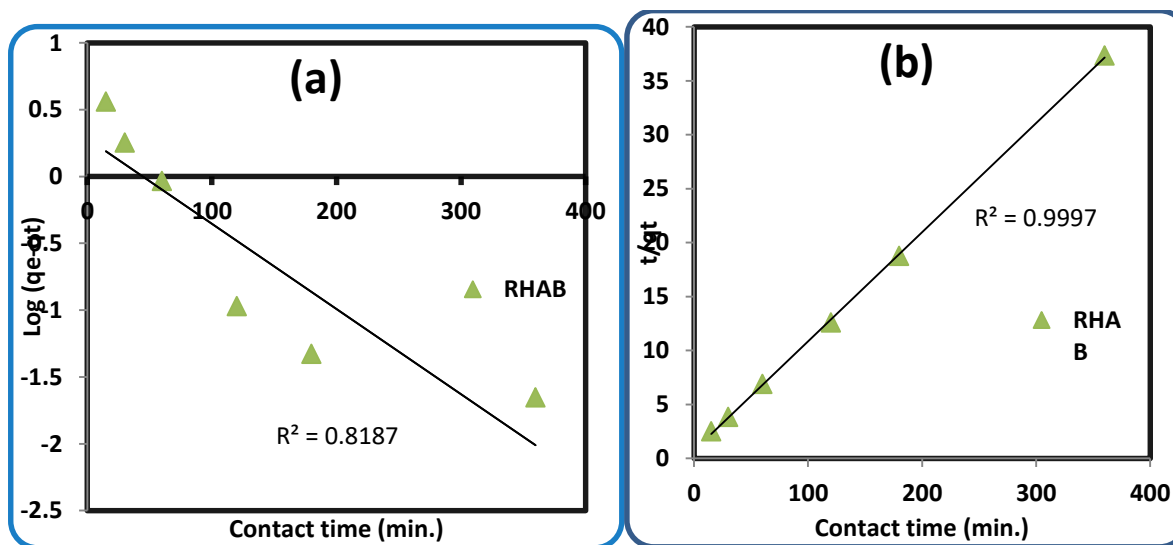


Fig. 12: Pseudo-first order (a) and Pseudo-second order (b) of kinetic models for the adsorption of Cu<sup>2+</sup> ions onto RHAB adsorbent respectively

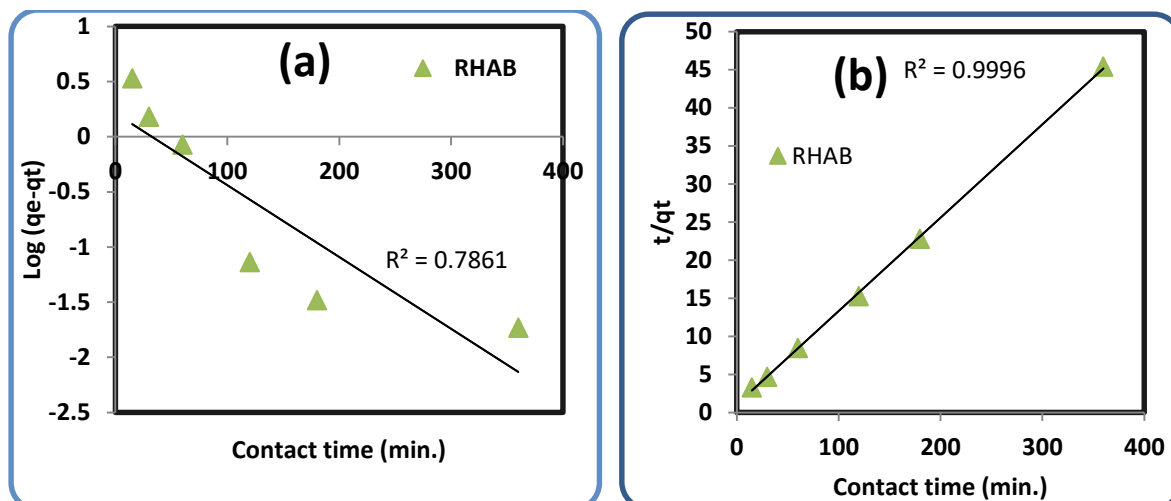


Fig. 13: Pseudo-first order (a) and Pseudo-second order (b) of kinetic models for the adsorption of  $\text{Ni}^{2+}$  ions onto RHAB adsorbent respectively

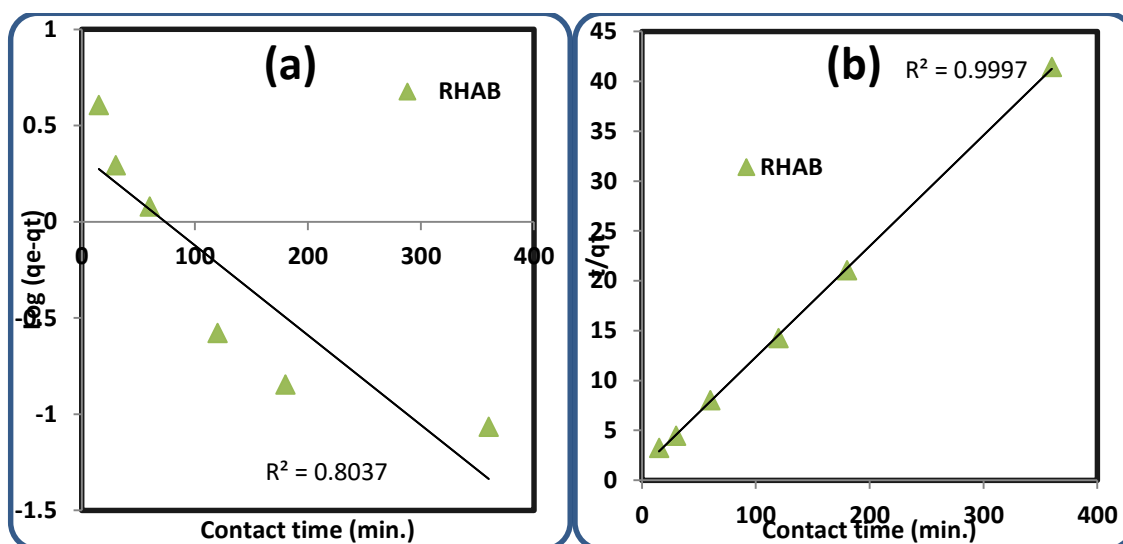


Fig. 14: Pseudo-first order (a) and Pseudo-second order (b) of kinetic models for the adsorption of  $\text{Mn}^{2+}$  ions onto RHAB adsorbent respectively.

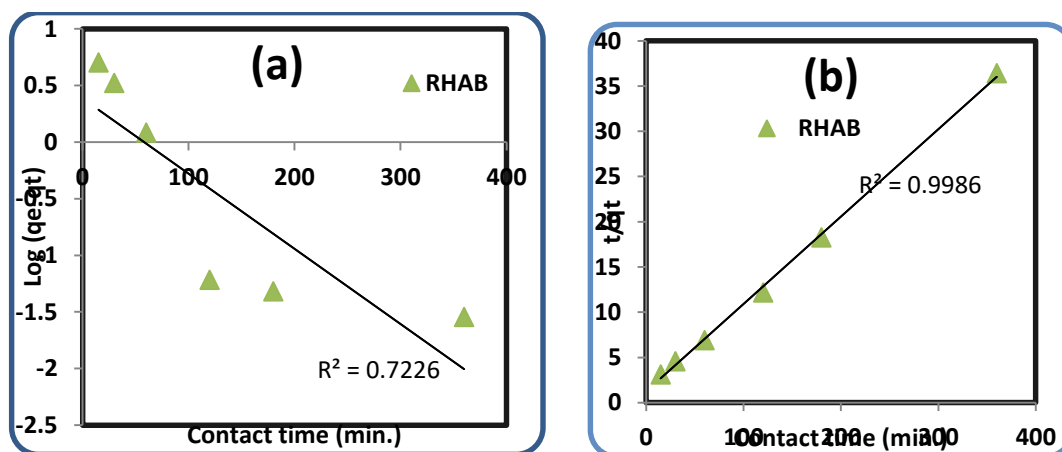
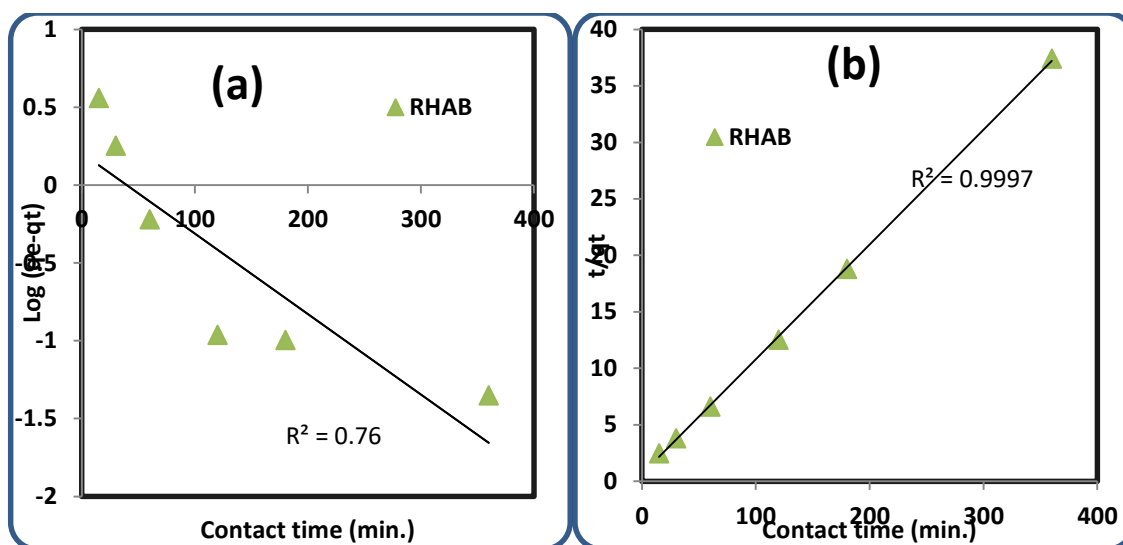


Fig. 15: Pseudo-first order (a) and Pseudo-second order (b) of kinetic models for the adsorption of  $\text{Pb}^{2+}$  ions onto RHAB adsorbent respectively.



**Fig. 16:** Pseudo-first order (a) and Pseudo-second order (b) of kinetic models for the adsorption of  $F^-$  ions onto RHAB adsorbent respectively.

Table 2 illustrates all the kinetic parameters of the two models at different contact time of adsorbate solution. It observed that the values of  $R_2$  and  $Q_{\max}$  of the pseudo-second-order kinetic model were better than the pseudo-first-order kinetic model for all elements absorbed in the surface of RHAB optimum

conditions. Therefore, it's more applicable to the kinetics adsorption of  $Cu^{2+}$ ,  $Ni^{2+}$ ,  $Mn^{2+}$ ,  $Pb^{2+}$  and  $F^-$  ions and therefore suggests a chemisorption process and the reactions are following the second order reaction.

**Table 2:** Illustrates the Pseudo-first order and Pseudo-second order of kinetic models for the adsorption of  $Cu^{+2}$ ,  $Ni^{+2}$ ,  $Mn^{+2}$ ,  $Pb^{+2}$ , and  $F^-$  onto RHAB adsorbent ( $n=3$ ).

Ions	Absorbent	Pseudo-first-order			Pseudo-second-order		
		qe	k1	R <sup>2</sup>	qe	k2	R <sup>2</sup>
$Cu^{2+}$	RHAB	1.921	0.0064	0.8187	9.891	0.0136	0.997
$Ni^{2+}$	RHAB	1.629	0.0065	0.7861	8.163	0.0144	0.9996
$Mn^{2+}$	RHAB	2.211	0.0047	0.804	8.993	0.001	0.9997
$Pb^{2+}$	RHAB	2.595	0.0066	0.723	10.35	0.0075	0.9986
$F^-$	RHAB	2.205	0.0052	0.76	9.843	0.016	0.997

### 3.8. Re-usability study

In order to check the reusability of the sorbent media, the used RHAB containing different heavy metals was firstly dried at  $50^\circ C$  for 3 hours, then treated with 0.1N HCl in jar test system at mixing rate 250 rpm for 2 hours and then tested again in the sorption unit under the conditions of the experiment that gave the best percentage removal of heavy metal ions from the aforementioned aqueous solution. The capacity of the sorbent for reuse was found to decrease until it became constant at a particular percentage of removal after a different number of times of repeated use as shown in fig. 17. The particular percentage removal

and the number of repeated uses were found to be dependent on the heavy metal. Thus, multiple uses of the sorbent were seen to be feasible. The bio-sorption process was carried out at optimum conditions for 3hour. It was observed that the effect of bio-sorption process of the re-used RHAB after acid treatment for maximum metal ion removal at constant dose 5 g/l, initial concentration 50 ppm, constant pH (5-5.5 and 2) for metal ions and  $F^-$ , respectively and mixing rate 160 rpm for 90 min. From fig. 17, it showed that; in optimum conditions of RHAB for maximum metal ion removal occurred at a constant dose (5 g/l)

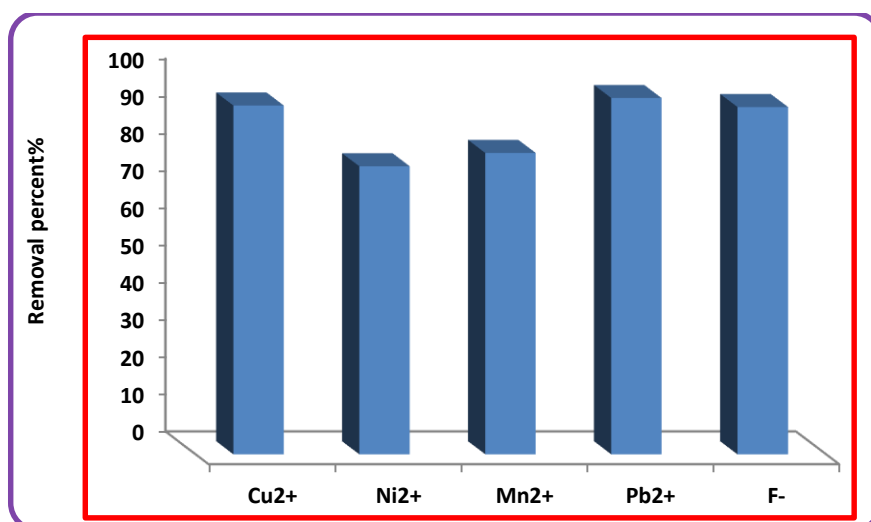


**Fig. 17:** Re-usability effect of bio-sorbent material after acid treatment on the percentage removal of Rhab for maximum metal ions and fluoride removal: (at T= 25°C, dose = 5 g/l, t = 60 min and pH (5-5.5 and 2) for metal ions and F<sup>-</sup>, respectively.

#### 4. CONCLUSION

RHAB showed a good ability to remove heavy metals and fluoride simulated synthesized aqueous solution. So, it can be recommended for the removal of heavy metal ions and fluoride from treatment plant wastewater instead of other materials such as activated carbon because it is valid, cheaper, economical, easier and simpler to use and has a high ability to adsorb heavy metal ions, can be used several times without the need for a costly regeneration method and finally can be further used for other beneficial uses. The maximum removal efficiency of heavy metal and fluoride ion were at optimum conditions with removal efficiencies 95, 78, 84, 98, 95 % for Cu<sup>2+</sup>, Ni<sup>2+</sup>, Mn<sup>2+</sup>, pb<sup>2+</sup> and F<sup>-</sup>, respectively at an initial concentration 50 ppm. The percentage removal of heavy metal and fluoride ions were increased with increasing the adsorbent dose of bio-sorbent material, initial concentration of heavy metal and fluoride ions, and the contact time at a constant mixing rate 160 rpm for both adsorbent materials. For the pH, the percentage removal, metal ions were increased with increasing pH for Cu<sup>2+</sup>, Ni<sup>2+</sup>, Mn<sup>2+</sup> and pb<sup>2+</sup>. While the percentage removal of F<sup>-</sup> ion was decreased with increasing pH of solutions.

#### Conflicts of interest

There are no conflicts to declare.

#### 5. Formatting of funding sources

No funding source.

#### 6. Acknowledgments

The authors acknowledge the central laboratory staff of Desert Research Center for their help for completing this study.

#### 7. References

- [1] Litidamu, N., T. Young, and I. Valemei. "An assessment of health impacts from environmental hazards in Fiji." *WHO, Fiji* (2003).
- [2] Oliveira J A, Cambraia J, Cano M A. Cadmium absorption and accumulation and its effects on the relative growth of water hyacinths and salvinia. *Rev Bras Fisiol Veg* 2001;13:329-41.
- [3] Reddy DH, Seshiah K, Reddy AVR, Rao MM, Wang MC. Biosorption of Pb<sup>2+</sup> from aqueous solutions by *Moringa oleifera* bark: Equilibrium and kinetic studies. *J Hazard Mater* 2010;174:831-8.
- [4] Krishna K, Satyanarayanan M, Govil PK. Assessment of heavy metal pollution in water using multivariate statistical techniques in an industrial area: a case study from Patancheru, Medak District, Andhra Pradesh, India. *J Hazard Mater* 2009;167:366–73.
- [5] Rapant S, Kr̃emov'a K. Health risk assessment maps for arsenic groundwater content: application of national geochemical databases. *Environ Geochem Health* 2007;29:131–4.
- [6] Sharma, G., Naushad, M., Kumar, A., Rana, S., Sharma, S., Bhatnagar, A., ... & Khan, M. R. (2017). Efficient removal of coomassie brilliant blue R-250 dye using starch/poly (alginic acid-cl-acrylamide) nanohydrogel. *Process Safety and Environmental Protection*, 109, 301-310.
- [7] Tran, H. N., You, S. J., Nguyen, T. V., & Chao, H. P. (2017). Insight into the adsorption mechanism of cationic dye onto biosorbents derived from agricultural wastes. *ChemicalEngineeringCommunications*, 204(9), 1020-1036.

- [8] Bhatnagar A, Sillanpää M, Witek-Krowiak A. Agricultural waste peels as versatile biomass for water purification—a review. *Chem Eng J* 2015; 270:244-71.
- [9] Yahya MA, Al-Qodah Z, Ngah CZ. Agricultural bio-waste materials as potential sustainable precursors used for activated carbon production. *Renew Sust Energ Rev* 2015;46: 218–35.
- [10] Pino GH, Souza LM, Torem ML Saavedra Pinto GA. Biosorption of cadmium by green coconut shell powder. *Miner Eng* 2006;19:380–7.
- [11] Ben-Ali S, Souissi-Najar S, Ouederni A. Characterization and adsorption capacity of raw pomegranate peel biosorbent for copper removal. *J Cleaner Prod* 2017;154:269–75.
- [12] Juang RS, Tseng RL, Wu FC, Lee SH. Adsorption behavior of reactive dyes from aqueous solutions on chitosan. *J Chem Technol Biotechnol* 1997;70:391–9.
- [13] Salmani MH, Miri M, Ehrampoush MH, Alahabadi A, Hosseini-Bandegharaei A. Comparing cadmium removal efficiency of a magnetized biochar based on orange peel with those of conventional orange peel and unmodified biochar. *Desalination Water Treat* 2017; 82:157–69.
- [14] Jafari AJ, Alahabadi A, Saghi MH, Rezai Z, Rastegar A, Zamani MS, et al. Adsorptive removal of phenol from aqueous solutions using chemically activated rice husk ash: equilibrium, kinetic, and thermodynamic studies. *Desalination Water Treat* 2019;158:233-44.
- [15] Singh T.P., Goel S., Majumder C. Biosorption of heavy metals by acclimated microbial species, acinetobacter baumannii, *Innovare J Life Sci* 2018;6:5–9.
- [16] Singh P, Raizada P, Pathania D, Sharma G, Sharma P. Microwave induced KOH activation of guava peel carbon as an adsorbent for congo red dye removal from aqueous phase. *Indian J Chem Technol* 2013;20:305–11.
- [17] Khan S, Raha ZF, Jabeen M, Rukh M, Reza ST, Khan EA. Removal of organic pollutant from aqueous solution by rice husk activated carbon (RHAC). *J Chem Eng* 2017;29:29–33.
- [18] Darabi S, Fatemeh S, Bahramifar N, Khalilzadeh MA. Equilibrium, thermodynamic and kinetics studies on adsorption of eosin Y and red X-GRL from aqueous solution by treated rice husk. *J Appl Res Wat Wastewater* 2018;5:392–8.
- [19] Sarkale P., Jadhav A. Utilization of rice husk and laterite as low-cost adsorbent for heavy metal removal through aqueous solution, *Innovare J Agric Sci* 2021;9:1–5.
- [20] Thakur C, Srivastava VC, Mall ID, Hiwarkar AD. Modelling of binary isotherm behaviour for the adsorption of catechol with phenol and resorcinol onto rice husk ash. *Indian Chem Eng* 2017;59:312–34.
- [21] Sudhakar P, Mall ID, Srivastava VC. Adsorptive removal of bisphenol-A by rice husk ash and granular activated carbon. *Desalination Water Treat* 2016;57:12375–84.
- [22] Mor S, Chhoden K, Ravindra K. Application of agro-waste rice husk ash for the removal of phosphate from the wastewater. *J Cleaner Prod* 2016;129:673–80.
- [23] Mittal A, Naushad M, Sharma G, Alotman Z, Wabaidur S, Alam M. Fabrication of MWCNTs/ThO<sub>2</sub> nanocomposite and its adsorption behavior for the removal of Pb (II) metal from aqueous medium. *Desalination Water Treat* 2016;57:21863–9.
- [24] Tarun KN, Ashim KB, Sailendranath M, Sudip KD. The sorption of lead (II) ions on rice husk ash. *J Hazard Mater* 2009;163:1254-6.
- [25] Nguyen TT, Ma HT, Avti P, Bashir MJ, Ng CA, Wong LY, et al. Adsorptive Removal of Iron Using SiO<sub>2</sub> Nanoparticles Extracted from Rice Husk Ash. *J Anal Methods*. 2019;2019:1-8. Article ID 6210240.
- [26] Bandhyopadhyay K, Das D, Bhattacharyya P, Maiti BR. Reaction engineering studies on bio-degradation of phenol by *Pseudomonas putida* MTCC 1194 immobilized on calcium alginate. *Bio-chem Eng J* 2001;8:179–86.
- [27] Domínguez A, Couto SR, Sanromán A. Dye decolorization by *Trametes hirsute* immobilized into alginate beads, *J Microbial Bio-technol* 2005;21:405-9.
- [28] Aziz N, Jayasuriya N, Fan L. Adsorption study on *Moringa oleifera* seeds and *Musa cavendish* as natural water purification agents for removal of Lead, Nickel and Cadmium from drinking water. *Mat Sci Eng* 2016;136:1-9.
- [29] Langmuir I. The constitution and fundamental properties of solids and liquids. *J Am Chem Soc* 1916;38(11):2221–95.
- [30] Freundlich H. Over the adsorption in solution. *J Phys Chem* 1906;57(385471):1100-7.
- [31] Lagergen S. About the theory of so-called adsorption of soluble substances. *Handlingar Band*.1898; 24(4):1-39.
- [32] Ho YS, McKay G. Pseudo-second order model for sorption processes. *Process Biochem* 1999;34:451–65.
- [33] Shu XZ, Zhu KJ, Song W. Novel pH-sensitive citrate cross-linked chitosan film for drug-controlled release. *Int J Pharm* 2011;212:19–28.
- [34] Chen G, Mi J, Wu X, Luo c, Li J, Tang y, et al. Structural features and bioactivities of the chitosan. *Int J Biol Macromol* 2011;49(4):543-7.
- [35] Patel M. potential of fruit and vegetable wastes as novel bio-sorbents: summarizing the recent studies. *Rev Environ Sci Biotechnol* 2012;11:365–80.
- [36] Farhaoui M, Derraz M. Optimizing coagulation process by using sludge produced in the water treatment plant. *J Chem Pharm Res* 2016;8:749-56.
- [37] Hongyuan L, Quanwaen R, Linghui X, Yan Z. Application of automatic control system in water plant in China. *J Converg Inf Technol* 2013;8(5):243-50.
- [38] Cayllahua JEB, Torem ML. Bio-sorption of aluminum ions onto *Rhodococcus opacus* from wastewaters. *Chem Eng J* 2010;161:1-8.
- [39] Pernitsky DJ. Coagulation 101, Associated Engineering, Calgary, Alberta, 2003; 17(2): 241-57.
- [40] Selvi K, Pattabhi S, Kadirvelu K. Removal of Cr (VI) from aqueous solution by adsorption onto activated carbon. *Biores Technol* 2001;80:87-9.
- [41] Hamadi NK, Chen XD, Farid MM, Lu MGQ. Adsorption kinetics for the removal of chromium(VI) from aqueous solution by adsorbents derived from used tyres and sawdust. *Chem Eng J* 2001;84:95-10.
- [42] Merzouk B, Gourich B, Madani K, Vial C, Sekki A. Removal of adisperse red dye from synthetic wastewater by chemical coagulation and continuous electrocoagulation. *Desalination* 2011;272:246-53.